Oecologia
https://doi.org/10.1007/s00442-022-05197-6

PHYSIOLOGICAL ECOLOGY – ORIGINAL RESEARCH

Bulk and amino acid nitrogen isotopes suggest shifting nitrogen balance of pregnant sharks across gestation

Oliver N. Shipley[1,5] · Jill A. Olin[2] · John P. Whiteman[3] · Dana M. Bethea[4] · Seth D. Newsome[1]

Received: 16 July 2021 / Accepted: 21 May 2022

Abstract

Nitrogen isotope ($\delta^{15}N$) analysis of bulk tissues and individual amino acids (AA) can be used to assess how consumers maintain nitrogen balance with broad implications for predicting individual fitness. For elasmobranchs, a ureotelic taxa thought to be constantly nitrogen limited, the isotopic effects associated with nitrogen-demanding events such as prolonged gestation remain unknown. Given the linkages between nitrogen isotope variation and consumer nitrogen balance, we used AA $\delta^{15}N$ analysis of muscle and liver tissue collected from female bonnethead sharks (*Sphyrna tiburo,* $n = 16$) and their embryos ($n = 14$) to explore how nitrogen balance may vary across gestation. Gestational stage was a strong predictor of bulk tissue and AA $\delta^{15}N$ values in pregnant shark tissues, decreasing as individuals neared parturition. This trend was observed in trophic (e.g., Glx, Ala, Val), source (e.g., Lys), and physiological (e.g., Gly) AAs. Several potential mechanisms may explain these results including nitrogen conservation, scavenging, and bacterially mediated breakdown of urea to free ammonia that is used to synthesize AAs. We observed contrasting patterns of isotopic discrimination in embryo tissues, which generally became enriched in ^{15}N throughout development. This was attributed to greater excretion of nitrogenous waste in more developed embryos, and the role of physiologically sensitive AAs (i.e., Gly and Ser) to molecular processes such as nucleotide synthesis. These findings underscore how AA isotopes can quantify shifts in nitrogen balance, providing unequivocal evidence for the role of physiological condition in driving $\delta^{15}N$ variation in both bulk tissues and individual AAs.

Keywords Shark · Nitrogen metabolism · Ecophysiology · Reproduction · Compound-specific isotope analysis

Introduction

The isotopic composition of individual compounds, such as amino acids (AA-SIA), are increasingly measured to provide a fine-scale understanding of animal ecology, including trophic relationships (McMahon and McCarthy, 2016; Ohkouchi et al. 2017) and energy flow (Larsen et al. 2009; McMahon et al. 2015; Skinner et al. 2021). Evidence is also accumulating for physiologically mediated patterns of isotopic fractionation within individual animals, driven by factors such as temperature dependence (Barnes et al. 2007), growth rate (Gorokhova 2018), dietary protein quality (Sponheimer et al. 2003; Whiteman et al. 2021a, b), and the sourcing of carbon and nitrogen from exogenous versus endogenous resource pools (Lübcker et al. 2020a, b; Whiteman et al. 2021a, b). Despite this growing body of literature, the role of animal physiology in driving patterns of isotopic variability remains underappreciated (Shipley and Matich 2020). For accurate interpretation of ecological patterns drawn from molecular isotope approaches, the physiological underpinnings of isotope variability require further empirical investigation in free-ranging animals.

AA-SIA holds great promise for tracing changes in the nutritional condition of organisms, particularly their nitrogen balance (O'Connell 2017; Whiteman et al. 2019). This technique leverages the distinct patterns of nitrogen isotope

Communicated by Donovan P German.

✉ Oliver N. Shipley
oshipley@unm.edu

[1] Department of Biology, University of New Mexico, Albuquerque, NM 87131, USA

[2] Biological Sciences, Great Lakes Research Center, Michigan Technological University, Houghton, MI 49931, USA

[3] Department of Biological Sciences, Old Dominion University, Norfolk, VA 23529, USA

[4] NOAA Fisheries Southeast Regional Office, Saint Petersburg, FL 33701, USA

[5] Beneath the Waves, PO Box 126, Herndon, VA 20172, USA

Published online: 20 June 2022

($\delta^{15}N$) discrimination among AAs, which reflect the biochemical pathways that link the AA to an organism's central pool of nitrogen (O'Connell 2017). This pool is dynamic and includes nitrogen waste products (e.g., ammonia) and metabolites like AAs (e.g., glutamate and glutamine) that routinely participate in trans- and deamination reactions. Thus, establishing longitudinal records of AA $\delta^{15}N$ values can provide insight into periods of fasting, nutritional stress, and perhaps reproduction (Lübcker et al. 2020a, b). From a nitrogen isotope perspective, AAs generally fall into one of three categories based on the extent of trans and de-amination (and thus ^{15}N fractionation) associated with assimilation and biosynthesis (McMahon and McCarthy 2016). Trophic AAs (e.g., Ala, Asx, Glx, Ile, Leu, Val, and Pro) are all tightly connected to the glutamate/glutamine pool, undergoing considerable trans- and deamination during metabolic processing, which results in considerable ^{15}N fractionation between consumer and diet. Source AAs (e.g., Phe, Tyr, Lys) undergo minimal trans- and deamination and exhibit low ^{15}N fractionation between consumer and diet, therefore reflecting the nitrogen baseline/s supporting animal biomass. Although the third category, physiological AAs (e.g., Gly, Ser, and Thr), are largely excluded from trans- and deamination with other AAs, they frequently exchange nitrogen between each other. This exchange can vary broadly with diet type and physiological condition, resulting in highly variable patterns of ^{15}N fractionation across taxa (Whiteman et al. 2019).

In practice, $\delta^{15}N$ values of AAs isolated from metabolically inert, but continuously growing tissues like whiskers (i.e., keratins) have been used to determine periods of fasting versus active foraging in southern elephant seals (*Mirounga leonina*; Lübcker et al. 2020b). While fasting, AAs closely associated with gluconeogenesis (e.g., Gly, Ser, Pro) had higher $\delta^{15}N$ values, patterns that were attributed to kinetic isotope fractionation associated with the deamination of AAs that are precursors for gluconeogenesis, as well as de novo synthesis of these non-essential AAs from endogenous tissue reserves (Lübcker et al. 2020b). A similar rationale has been used to assess capital versus income breeding strategies in seabirds (Whiteman et al. 2021a, b), where the isotopic fractionation associated with the biochemical steps required for tissue catabolism in capital breeding in emperor penguins (*Aptenodytes forsteri*) stood in clear contrast from the income breeding of herring gulls (*Larus argentatus smithsonianus*; Hebert et al. 2016). These recent studies illustrate the capacity of AA-SIA for tracing nitrogen balance strategies during important life history events. Such studies are increasingly pertinent, because both physiological and ecological processes should be considered in tandem when interpreting bulk and AA isotope patterns.

Nitrogen balance is of particular interest in the study of elasmobranch fishes (sharks, skates, and rays), one of the most speciose vertebrate groups with an evolutionary lineage extending back over ~400 million years (Stein et al. 2018). This extensive phylogenetic history encapsulates a diverse array of reproductive strategies ranging from strict ovipary (egg laying) to a gradient of vivipary (live birth) (Conrath and Musick 2012). Elasmobranchs are unique because despite their largely carnivorous diet, they appear to be one of the most nitrogen-limited aquatic vertebrates (Wood and Giacomin 2016; Ballantyne 2016; Wood et al. 2019), owing to the unique high nitrogen demand relative to other fishes for urea-based osmoregulation (Smith 1936). This demand may be especially acute for omnivorous elasmobranchs, which have relatively low dietary nitrogen input (e.g., Leigh et al. 2018). Due to this comparatively high demand for nitrogen, elasmobranchs have a strong need to maintain their nitrogen balance during periods of high nutritional stress. For example, they can scavenge nitrogenous compounds (e.g., ammonia) directly through the gills, which can be routed to protein synthesis (Wood and Giacomin 2016). Additionally, symbiotic bacteria that possess the urease enzyme and are found ubiquitously across elasmobranch tissues can convert isotopically light urea to free ammonia during periods of elevated nutritional stress (Wood et al. 2019). From an isotopic perspective, these nitrogen balance strategies may significantly alter the $\delta^{15}N$ values of both bulk tissue and individual AAs, confounding clear ecological interpretation across potentially hundreds of taxa. Furthermore, the unique nitrogen metabolism of this group is likely especially important during reproduction, as most elasmobranchs are characterized by long gestation periods (Cortés 2000; Frisk et al. 2005; Dulvy et al. 2014), which likely incur high nitrogen demand. Despite this, patterns of isotopic discrimination throughout elasmobranch gestation remain almost entirely unknown.

Here, we explore $\delta^{15}N$ values in bulk tissues and their constituent AAs collected from pregnant bonnethead sharks (*Sphyrna tiburo*) and their embryos. This viviparous species exhibits a hybrid mode of embryonic resource allocation, where during early gestation (3–4 months) embryos are reliant upon an egg yolk before forming an egg-yolk placenta when reaching ~ 9–10 cm in length (Schlernitzauer and Gilbert 1966; Olin et al. 2018). We predicted that during the late, egg-yolk placenta stage of gestation, (1) bulk and AA $\delta^{15}N$ values of liver and muscle tissues in pregnant females will decline, owing to increased retention and/or mobilization of ^{14}N during periods of high nutritional demand (Fuller et al. 2004; Clark et al. 2016; Lübcker et al. 2020a), and 2) $\delta^{15}N$ values of embryo tissues will increase relative to their mothers (McMeans et al. 2009; Olin et al. 2011, 2018), owing to increased excretion of ^{15}N-depleted nitrogenous waste products (e.g., urea) and de novo synthesis of non-essential AAs. This study aims to shed new light on the ecophysiological drivers of isotopic variability in free

ranging animals, adding a new dimension to the interpretation of bulk and compound-specific isotopic data.

Materials and methods

Field sampling

Mature female bonnethead sharks were opportunistically sampled during the NOAA Fisheries Gulf of Mexico Shark Pupping and Nursery fishery-independent survey. Samples were collected from four locations in the eastern US Gulf of Mexico from April through September 2012–2015: St Andrew Bay, Crooked Island Sound, St Joseph Bay, and the gulf-side of St Vincent Island, FL (Fig. 1, Bethea et al. 2007). Sharks were collected with gillnets of different stretch-mesh sizes (following Carlson and Brusher 1999) ranging from 7.6 cm (3.0″) to 14.0 cm (5.5″) in steps of 1.3 cm (0.5″). Each panel was 3.0 m (10 ft) deep and 30.5 m (100 ft) long. Panel specifics can be found in Baremore and Hale (2012). The six panels were strung together and fished as a single gear for up to 1 h (set). Up to five sets were made at each location per month. In the field, pre-caudal, fork, and stretch total length (cm), sex, life stage (immature, mature) was determined. Mature females relatively unaffected by capture were tagged and released (following Bethea et al. 2016) and those suffering extensive injury during capture were euthanized for this study. Euthanized animals were placed on ice until further processing. Individuals in a range of gestational stages were captured across all sampling locations to constrain any potential impacts of geographic variation in isotope baselines on shark tissue AA isotope values.

Upon returning to the NOAA Fisheries Panama City Laboratory, total weight (kg), liver weight (g), and the number of corresponding embryos in both the left and right uteri of each adult were recorded. To account for the effect of shark body size on liver weights across individuals, adult liver weights were normalized by dividing by the fork length. Approximately 2 g of muscle (from above the spine, anterior to the first dorsal fin) and liver tissue was collected from each adult and immediately placed frozen at −4 °C. When present, each individual embryo (whole body) was separated from its corresponding yolk-sac placenta and yolk, measured for fork length (cm), weighed (g) and sexed, where possible. The yolk-sac placenta is defined here as (1) the egg envelope that surrounds each of the embryos, (2) the associated umbilical stalks, and (3) the vascularized portions attached to the uterine wall (Hamlett et al. 2005). Embryos were immediately frozen at −4 °C. For larger embryos (> 9 cm total length), 1–2 mg of liver tissue was excised and frozen at −4 °C. Frozen samples were shipped on dry ice for further preparation of bulk tissue and amino acid isotope analysis.

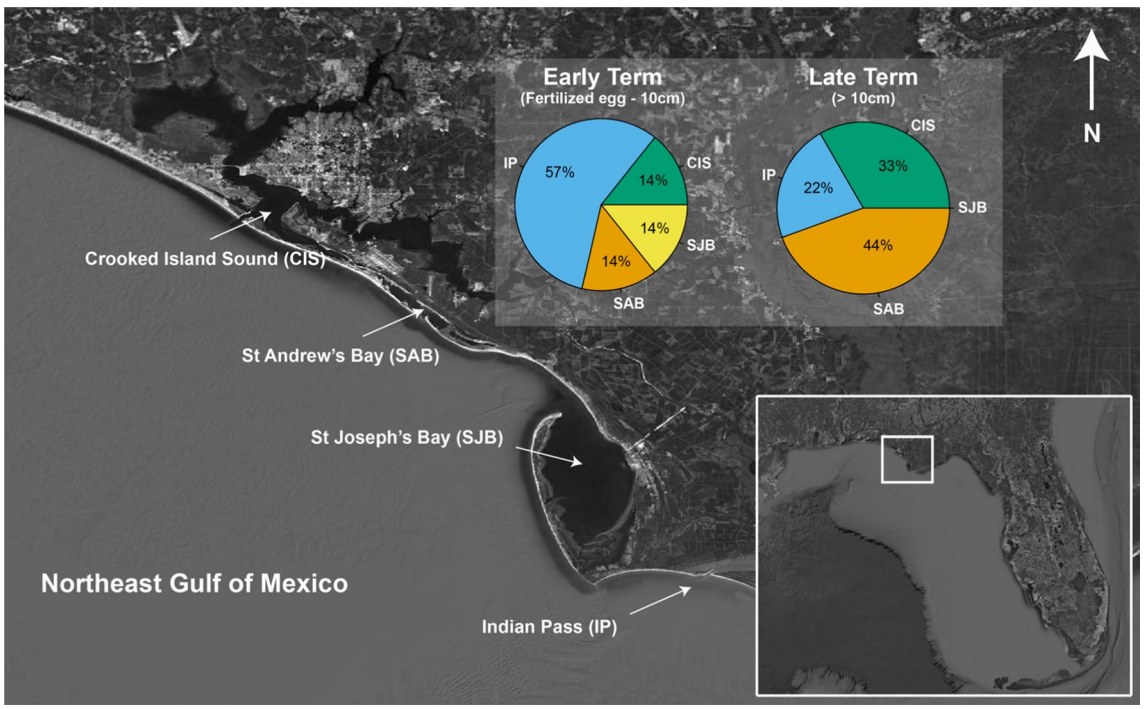

Fig. 1 Sampling locations for mature female bonnethead sharks used in this study. Top right inset highlights the percentage of early- and late-term individuals sampled across the four capture locations: *CIS* Crooked Island Sound, *SAB* St Andrew's Bay, *SJB* St Joseph's Bay, *IP* Indian Pass (St. Vincent's Island). Bottom right inset illustrates sampling region relative to the Florida pan handle and wider northeast Gulf of Mexico. Source: The Northeast Gulf of Mexico, Google Earth, Accessed 27th May 2021

Stable isotope analysis

We quantified bulk and AA $\delta^{15}N$ values for liver and muscle tissue of 16 pregnant bonnethead sharks. From these individuals we also analyzed two fertilized eggs, four whole body embryos (early-term), and liver tissue from eight larger embryos (late-term). Samples were freeze dried and vortexed three times with DI water to remove ^{15}N-depleted nitrogenous compounds, such as urea and trimethylamine *n*-oxide (Carlisle et al. 2017; Shipley et al. 2017a). Samples were also immersed in 2:1 chloroform methanol (Folch 1957) for 72 h, replacing the solvent solution every 24 h to remove lipids (Hussey et al. 2012) and dried at 50 °C.

Approximately 0.5–0.7 mg of dried tissue was then weighed into tin capsules for bulk tissue stable isotope analysis. Bulk nitrogen isotope ($\delta^{15}N$) values were measured with a Costech ECS 4010 Elemental Analyzer coupled to a Thermo Scientific Delta V Plus isotope ratio mass spectrometer via a CONFLO IV interface (EA-IRMS) at the University of New Mexico Center for Stable Isotopes (UNM-CSI; Albuquerque, NM). Isotope values are reported using the standard delta (δ) notation relative to V-AIR. Three internal laboratory standards were run at the beginning, at intervals between samples, and at the end of analytical sessions. Analytical precision calculated from repeat measurement of standards was ± 0.1‰ (1 σ). Analyses were normalized to three laboratory standards, which were calibrated against international certified reference standards of IAEA N1, IAEA N2 and USGS 43. The three internal laboratory standards were casein (Sigma Aldrich, $\delta^{15}N = 6.4‰$), soy (Sigma Aldrich, $\delta^{15}N = 1.0‰$), and tuna protein (University of New Mexico, $\delta^{15}N = 13.3‰$).

For isotopic analysis of individual amino acids, ~ 10–20 mg of dried tissue was hydrolyzed by immersing each sample in 1 ml of 6 N HCL at 110 °C for 20 h. This process converts glutamine to glutamic acid (Glx) and asparagine to aspartic acid (Asx). Samples were then cooled and dried down to a fine film under a gentle stream of N_2 gas. The remaining hydrolysate was derivatized to N-trifluoroacetic acid isopropyl esters (Silfer et al. 1991) Prior to analysis, samples were immersed in dichloromethane (DCM) and dried under a gentle stream of N_2 gas; this process was repeated twice. After the second DCM rinse, each sample was suspended in 50–150 ml of DCM and 1µL of sample was injected onto a Thermo Scientific Trace 1310 gas chromatograph for AA separation, then combusted/reduced at 1000 °C to N_2 with a Thermo Scientific IsoLink II coupled to a Thermo Scientific Delta V Plus isotope ratio mass spectrometer at UNM-CSI. All samples were run as duplicate injections, bracketed by two injections of an in-house standard where the isotopic composition of each AA was known and measured via EA-IRMS. Because derivatization does not add nitrogen atoms to each AA, samples were corrected following:

$$\delta^{15}N_{USA} = (\delta^{15}N_{DSA} + (\delta^{15}N_{DST} - \delta^{15}N_{UST})), \quad (1)$$

where $\delta^{15}N_{USA}$ represents the $\delta^{15}N$ value of the underivatized sample, $\delta^{15}N_{DSA}$ is the measured $\delta^{15}N$ value for a derivatized sample, $\delta^{15}N_{DST}$ is the accepted $\delta^{15}N$ value of the derivatized standard, and $\delta^{15}N_{UST}$ is the known $\delta^{15}N$ value of the underivatized standard. $\delta^{15}N$ values are presented for 13 AAs (here, by order of separation): Ala, Gly, Thr, Ser, Val, Leu, Ile, Pro, Asx, Glx, Phe, Tyr, and Lys. Known $\delta^{15}N$ values of powdered AA standards (Sigma Aldrich, Saint Louis, MO USA) measured via EA-IRMS are reported in the supplementary information (Appendix S1; Table S1. Within-run average analytical error (SD) for each individual-derived AA measured via GC–C–IRMS was: Ala = 0.5‰, Gly = 0.5‰, Thr = 0.3‰, Ser = 0.4‰, Val = 0.3‰, Leu = 0.4‰, Ile = 0.4‰, Pro = 0.2‰, Glx = 0.4‰, Phe = 0.4‰, Tyr = 0.4‰, Lys = 0.3‰ ($n = 24$ runs, Appendix S1: Table S1).

Quantitative analyses

All statistical analyses were run in the programming software R (v 4.0.0) using the Rstudio interface. All data were examined for normality and heteroscedasticity using Shapiro–Wilks and *F* tests, respectively. Statistical significance, α was 0.05.

Drivers of bulk and AA δ.[15] N values in pregnant bonnethead sharks

Mature female bonnethead sharks were categorized into two major gestational stages: early- and late-term individuals. Early-term females ($n = 7$) had fertilized eggs or embryos with an average fork length < 9 cm; these embryos likely rely upon egg yolk for nutrition. Late-term females ($n = 9$) had embryos > 9 cm fork length, which provides a conservative estimate as to when a yolk-sac placenta is partially or fully established (Schlernitzauer and Gilbert 1966; Olin et al. 2018).

Generalized linear models (GLMs) fit with a Gaussian error distribution were used to investigate the drivers of $\delta^{15}N$ values of bulk tissue and individual AAs. Predictor variables, which were considered fixed effects, included fork length of pregnant females (FL_{Mom}), liver weight:total weight of pregnant females (w), average embryo length (FL_{Embryo}), and total number of embryos ($N_{Embryos}$). We also included the interaction between FL_{Mom}*w. A full definition of predictor variables can be found in Table 1. We used stepwise forward–backward selection of non-significant

Table 1 Description and justification of predictor variables used in generalized linear models predicting variation in bulk tissue and amino acid $\delta^{15}N$ values of pregnant female bonnethead sharks

Predictor	Denotation	Units	Description and justification	References
Mother fork length	FL_{Mom}	Centimeters	Standard length measurement used for fishes typically refers to a linear measurement from the top of the rostrum to the fork of the caudal fin. Often used as a proxy for life history stage, which can be a significant predictor of animal $\delta^{15}N$ values due to ontogenetic diet shifts	Galvan et al. (2010); Estrada et al. (2006); Matich et al. (2019)
Liver weight: total body weight (pregnant females)	w	N/A	Due to the potential for liver catabolism during periods of elevated nutritional stress, we hypothesized that liver mass may be reduced in later-term individuals. Liver weight was normalized to total body weight to account for body size-based differences in liver mass	Widdowson (1976); Hobson et al. (1993); Graves et al. (2012); Lee et al. (2012)
Average embryo length	FL_{Embryo}	Centimeters	The average fork length of all embryos excised from the uteri of the corresponding pregnant female shark. Here, FL_{Embryo} is used as a proxy for gestational stage as embryo size is a strong predictor for when the yolk-sac placenta is formed	Schlernitzauer and Gilbert (1966); Olin et al. (2018)
Number of embryos	$N_{Embryos}$	Count	We hypothesized that a larger number of embryos may elicit higher nutritional demand on pregnant female sharks throughout gestation, potentially impacting $\delta^{15}N$ values	Leon and Woodside (1983); Kounig et al. (1988)

effects and determined the most parsimonious model using Akaike's information criterion (AIC).

Finally, we examined differences in four trophic–source AA pairs previously used to predict mobilization of endogenous nitrogen to support egg growth ($\Delta^{15}N_{Glx\text{-}Phe}$, $\Delta^{15}N_{Glx\text{-}Lys}$, $\Delta^{15}N_{Pro\text{-}Phe}$, $\Delta^{15}N_{Pro\text{-}Lys}$, Whiteman et al. 2021a, b) between early- and late-term females using pairwise comparisons (Student's t tests or Wilcoxon tests based on normality and heteroscedasticity).

Drivers of bulk and AA δ.[15] N values in bonnethead shark embryos

We examined relative changes to embryo AA and bulk tissue isotope values across four developmental stages: fertilized egg (egg yolk with no obvious developing embryo, $n = 2$), early-term (full body embryo tissue, average embryo fork length < 5 cm, $n = 4$), mid-term (embryo liver tissue, average embryo fork length = 9 – 11 cm, $n = 4$), and late-term embryos (embryo liver tissue, average embryo fork length = 19 – 24 cm, $n = 4$). We adopted these categorizations based on the relatively low sample sizes coupled with the different tissues analyzed from each developmental stage.

Fertilized egg tissue was sampled from two unique mothers. For each developmental stage of embryos, two embryos were sampled per pregnant female to account for within-uteri isotopic variability (McMeans et al. 2009; Olin et al. 2018). Nitrogen isotopic offsets (bulk tissue and AAs) between mothers and their corresponding embryos ($\Delta^{15}N_{Mother\text{-}Embryo}$) were calculated. Due to low sample sizes, we were unable to statistically compare isotopic differences among groups; instead, we describe general trends based on mean isotope values for each developmental group.

Next, we examined how relative offsets between trophic source pairs ($\Delta^{15}N_{Glx\text{-}Phe}$, $\Delta^{15}N_{Glx\text{-}Lys}$, $\Delta^{15}N_{Pro\text{-}Phe}$, $\Delta^{15}N_{Pro\text{-}Lys}$) changed in embryo tissues throughout their development. For individuals at each developmental mode, $\Delta^{15}N_{Glx\text{-}Phe}$, $\Delta^{15}N_{Glx\text{-}Lys}$, $\Delta^{15}N_{Pro\text{-}Phe}$, and $\Delta^{15}N_{Pro\text{-}Lys}$ were normalized to the value of corresponding offsets in fertilized egg tissue using the following approach. First, we calculated these offsets for fertilized egg tissue ($n = 2$). Second, we evaluated how these offsets changed throughout embryonic development using this formula: [Embryo $\Delta^{15}N_{TrophicAA\text{-}SourceAA}$] – [fertilized egg $\Delta^{15}N_{TrophicAA\text{-}SourceAA}$]. For example, if $\Delta^{15}N_{Glx\text{-}Phe}$ for mid-term embryo liver tissue ($n = 4$) was identical to $\Delta^{15}N_{Glx\text{-}Phe}$ for fertilized egg tissue, the normalized $\Delta^{15}N_{Glx\text{-}Phe}$ would be 0‰, indicating that there was no change in this

offset during development from fertilized egg to midterm embryo. We quantified changes in relative offsets between $\Delta^{15}N_{TrophicAA\text{-}SourceAA}$ across embryo development (defined here as FL_{Embryo}, see Table 1) using linear regressions.

Results

Generally, bulk tissue and AA $\delta^{15}N$ values were highest in the muscle tissue of pregnant females, and lowest in mother liver and fertilized egg tissues (Fig. 2). Across all tissues, the greatest range of AA $\delta^{15}N$ values was observed in Ala (11.5‰), Asx (11.2‰), Gly (13.8‰), Ser (10.1‰), and Thr (14.4‰, Fig. 2).

Drivers of bulk and AA δ.^{15} N values in pregnant bonnethead sharks

After stepwise selection, FL_{Embryo} was the most common significant predictor of pregnant female muscle and liver $\delta^{15}N$ values across bulk tissue and trophic and source AAs (Table 2, Fig. 3); in general, $\delta^{15}N$ values of pregnant females declined with increasing FL_{Embryo}. Second, $N_{Embryos}$ and w were often included in best fit models, with $N_{Embryos}$ often positively related to $\delta^{15}N$ values (Table 2, Fig. 3). Relationships between w and $\delta^{15}N$ values were both positive (for trophic AAs) and negative (for physiological and source AAs); however, in most models both $N_{Embryos}$ and w were not statistically significant (Table 2, Fig. 3).

For muscle tissue of pregnant females, $\Delta^{15}N_{Glx\text{-}Lys}$ was higher in early-term ($\Delta^{15}N_{Glx\text{-}Lys} = 17.0 \pm 0.6$‰) compared to late-term individuals ($\Delta^{15}N_{Glx\text{-}Lys} = 16.0 \pm 0.7$‰) ($t$ test, $t = 3.233$, $p = 0.006$, Fig. 4). The remaining trophic–source pairs did not differ between early- and late-term individuals. For liver tissue, $\Delta^{15}N_{Glx\text{-}Phe}$ was significantly higher in early-term ($\Delta^{15}N_{Glx\text{-}Phe} = 13.7 \pm 0.4$‰) than in late-term individuals ($\Delta^{15}N_{Glx\text{-}Phe} = 12.3 \pm 1.5$‰) (Wilcoxon test, $W = 51$, $p = 0.042$, Fig. 4; top panels). This was predominantly driven by a decrease in $\delta^{15}N_{Glx}$ values in late-term individuals (Fig. 4; bottom panels). The remaining trophic–source pairs did not differ between early- and late-term individuals. The $\delta^{15}N$ value declined with FL_{Embryo} for a single AA in muscle (Glx) and for three AA in liver (Glx, Pro, Lys; Fig. 4; bottom panels).

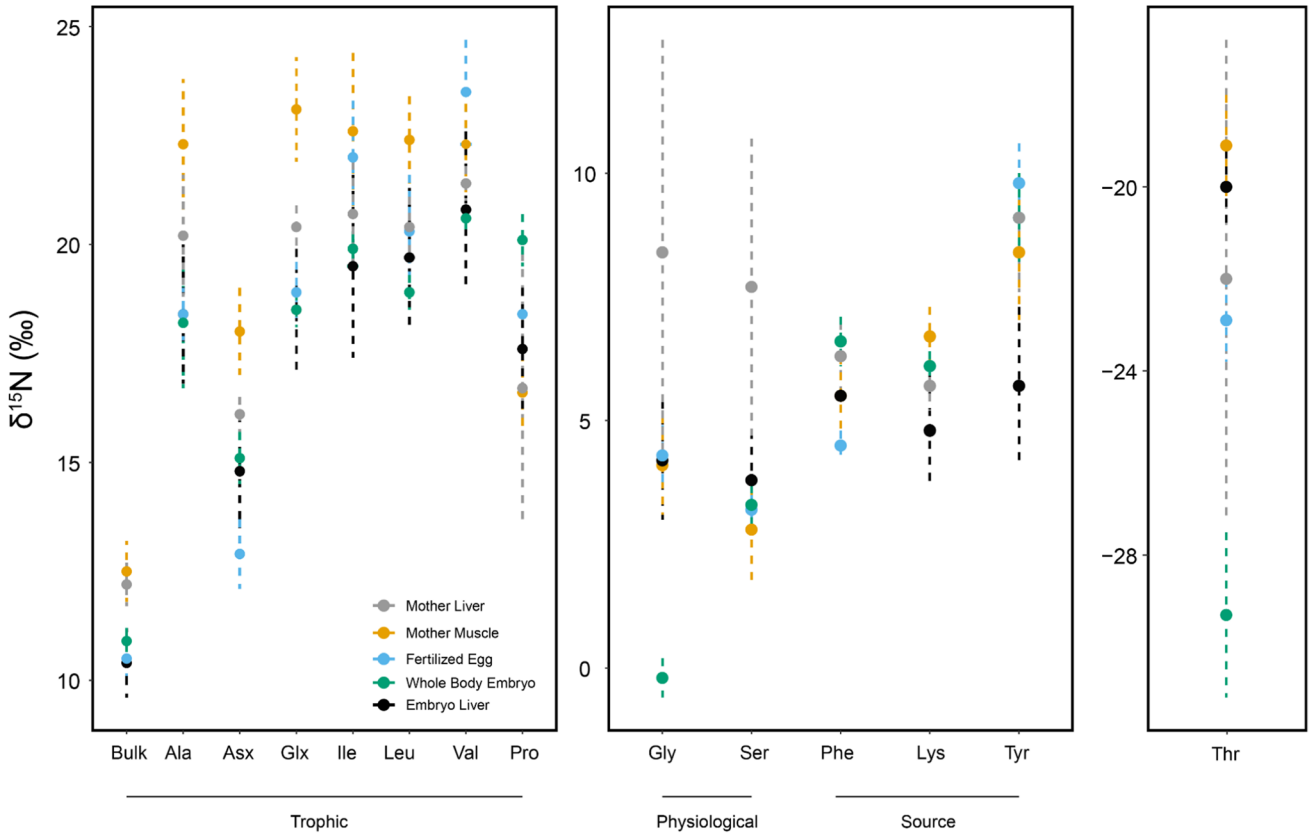

Fig. 2 Mean (±1 SD) bulk tissue and amino acid nitrogen isotope ($\delta^{15}N$) values for bonnethead shark muscle and liver tissue ($n = 16$) and corresponding fertilized egg ($n = 2$), whole body embryos ($n = 4$), and large embryo liver tissue ($n = 8$). Amino acids are grouped based on their relative application in ecological and ecophysiological studies (Whiteman et al. 2018)

Table 2 Model coefficients (p values) derived from generalized linear models investigating the drivers of bulk and amino acid $\delta^{15}N$ values in the muscle and liver tissue of pregnant female bonnethead sharks. ΔAIC represents the difference in AIC values between full and reduced models. Bold indicates statistical significance at alpha = 0.05*, 0.01** and 0.001*** levels

Amino acid	Group	Intercept	FL_{Mom}	FL_{Embryo}	$N_{Embryos}$	Weight	FL_{Mom}[a]w	ΔAIC
Muscle								
Bulk	–	**17.561 (< 0.001***)**	**−0.077 (0.027a)**	**−0.058 (0.013*)**	0.059 (0.143)	**0.340 (0.041*)**	–	1.147
Ala	Trophic	**20.503 (< 0.001***)**	–	**−0.132 (0.020)**	**0.198 (0.046*)**	0.406 (0.185)	–	2.93
Asp	Trophic	**18.052 (< 0.001***)**	–	**−0.107 (0.007**)**	0.114 (0.098)	–	–	3.898
Glu	Trophic	**22.973 (< 0.001***)**	–	**−0.118 (0.018*)**	0.162 (0.078)	–	–	3.991
Ile	Trophic	**22.935 (< 0.001***)**	–	**−0.202 (0.003**)**	0.183 (0.110)	–	–	3.955
Leu	Trophic	**22.252 (< 0.001***)**	–	−0.089 (0.008**)	–	0.252 (0.187)	–	3.619
Val	Trophic	**23.086 (< 0.001***)**	–	**−0.096 (0.048*)**	–	–	–	4.522
Pro	Trophic	**14.369 (< 0.001***)**	–	–	0.107 (0.098)	0.411 (0.057)	–	3.788
Gly	Physiological	**29.368 (0.028*)**	−0.283 (0.067)	−0.058 (0.145)	–	−6.601 (0.061)	0.074 (0.067)	1.999
Ser	Physiological	23.555 (0.100)	−0.197 (0.231)	−0.062 (0.180)	-0.130 (0.154)	**−8.657 (0.039*)**	**0.095 (0.047*)**	0
Phe	Source	**5.513 (< 0.001***)**	–	–	–	–	–	5.752
Lys	Source	**18.334 (0.050*)**	−0.144 (0.180)	–	–	−3.257 (0.176)	0.040 (0.154)	1.496
Tyr	Source	**8.415 (< 0.001***)**	–	**−0.129 (0.031*)**	0.146 (0.185)	–	–	4.674
Thr	–	**−17.694 (< 0.001***)**	–	0.062 (0.167)	-0.105 (0.196)	−0.324 (0.216)	–	3.747
Liver								
Bulk	–	**25.999 (0.006**)**	−0.174 (0.083)	**−0.098 (0.002**)**	–	−3.782 (0.095)	0.044 (0.093)	0.374
Ala	Trophic	**17.462 (< 0.001***)**	0.398 (0.091)	**−0.179 (0.002**)**	0.131 (0.127)	0.400 (0.151)	–	3.61
Asp	Trophic	**13.713 (< 0.001***)**	–	–	0.151 (0.130)	–	–	6.405
Glu	Trophic	**19.101 (< 0.001***)**	–	**−0.199 (< 0.001***)**	**0.142 (0.030*)**	–	–	5.598
Ile	Trophic	**21.226 (< 0.001***)**	–	**−0.2031 (0.007**)**	–	–	–	5.168
Leu	Trophic	**20.457 (< 0.001***)**	–	**−0.202 (< 0.001***)**	0.130 (0.124)	–	–	2.365
Val	Trophic	**21.664 (< 0.001***)**	–	**−0.225 (0.001***)**	0.144 (0.190)	–	–	5.479
Pro	Trophic	**22.499 (< 0.001***)**	−0.068 (0.171)	**−0.168 (< 0.001***)**	**0.269 (0.003**)**	–	–	2.386
Gly	Physiological	**5.022 (< 0.001***)**	–	**−0.097 (0.025*)**	–	–	–	5.556
Ser	Physiological	23.555 (0.100)	−0.200 (0.231)	−0.062 (0.180)	−0.129 (0.154)	**−8.657 (0.039*)**	**0.095 (0.047*)**	0
Phe	Source	**5.527 (< 0.001[c])**	–	–	–	–	–	6.504
Lys	Source	**12.545 (0.012[a])**	−0.120 (0.075)	**−0.091 (0.044*)**	0.136 (0.098)	0.447 (0.161)	–	1.37
Tyr	Source	**7.039 (< 0.001[c])**	–	**−0.156 (0.005**)**	–	–	–	6.195
Thr	-	**−33.931 (< 0.001[c])**	0.146 (0.122)	–	–	**6.200 (0.008**)**	**−0.069 (0.011*)**	1.856

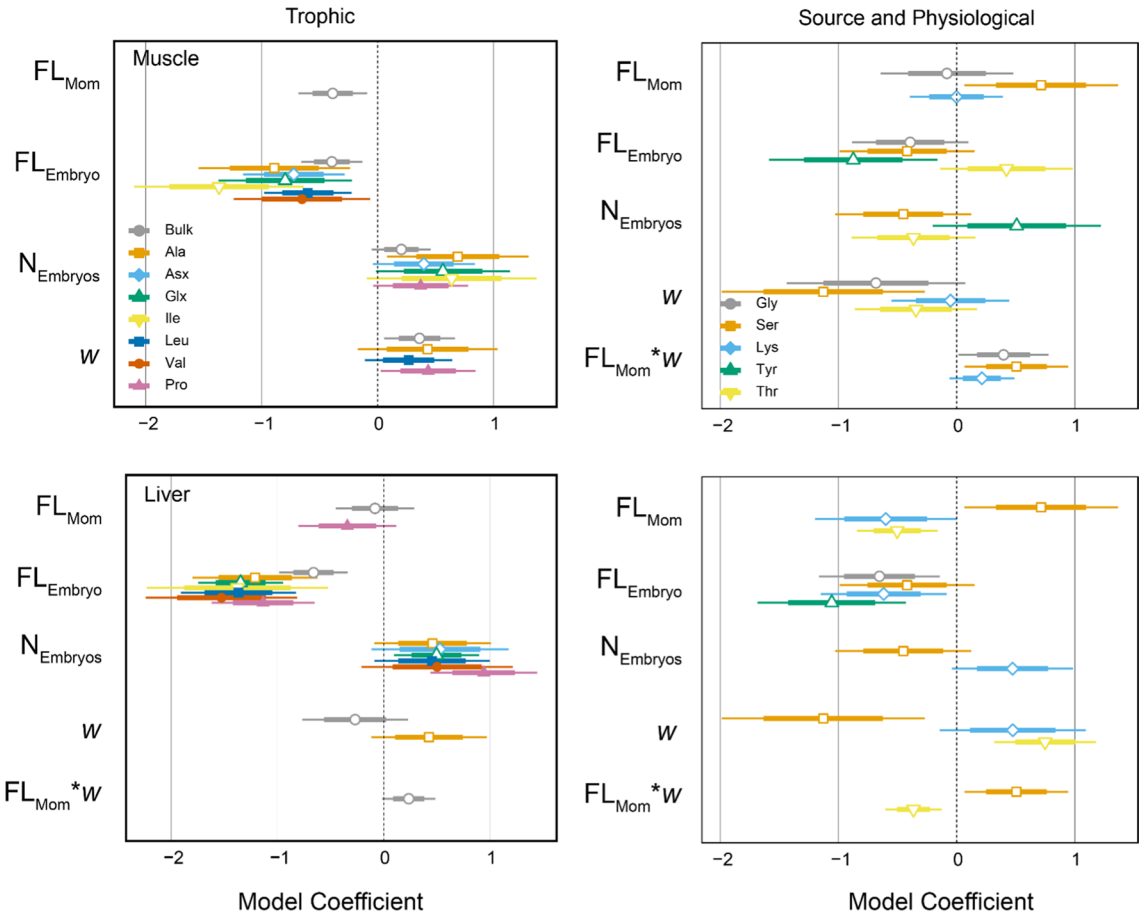

Fig. 3 Model coefficients for best fitted generalized linear models exploring the drivers of bulk tissue and amino acid $\delta^{15}N$ values for pregnant female bonnethead shark muscle (top panels) and liver (bottom panels) tissue. Predictors include fork length (FL) of pregnant females and their embryos (FL_{Mom}, FL_{Embryo}), total number of embryos ($N_{Embryos}$), the ratio of pregnant female liver mass to body mass (w), and an interaction term. Left panels show bulk tissue and trophic amino acids, right panels show physiological and source amino acids (including Thr). Horizontal bars represent 95% (thin lines) and 75% (thick lines) confidence intervals for model coefficients

Drivers of bulk and AA δ^{15}N values in bonnethead shark embryos

Changes in nitrogen metabolism during gestation were also reflected in embryo tissue (Fig. 5). Generally, $\delta^{15}N$ values of trophic and physiological AAs (and Thr) increased between early- and late-term embryos, a trend that was also reflected in bulk tissue, while $\delta^{15}N$ values of source AAs remained fairly constant (Fig. 5). Three trends stood out for late-term embryos in particular: a dramatic decline in $\delta^{15}N$ values of Pro (> 6‰), dramatic increases in Gly and Ser (> 6‰), and a convergence in which the mean $\delta^{15}N$ values for most trophic AAs (Ala, Glx, Ile, Leu, Val) fell from ~ 5‰ for fertilized eggs to ~ 1‰ for late-term embryos.

Changes in offsets between mothers and corresponding embryos (i.e., $\Delta^{15}N_{Mother\text{-}Embryo}$) generally decreased with development stage, and in many cases negative offsets were observed (Fig. 6). Offsets were more pronounced between liver tissue relative to muscle (Fig. 6), with most embryo AA $\delta^{15}N$ values becoming considerably higher (~ 4‰) relative to corresponding mothers during later development (Fig. 6). Notably, embryo Gly and Ser $\delta^{15}N$ values became enriched by > 8‰ relative to mother liver tissue $\delta^{15}N$ values in the late-term individuals. One exception was $\delta^{15}N$ values of Pro, which became higher in mother tissues relative to embryos during late gestation (Figs. 5 & 6), this pattern was also reflected in trophic–source pairs of embryo tissues (Fig. 7A).

The offsets of $\Delta^{15}N_{Trophic\ AA\text{-}Source\ AA}$ for embryo tissues, normalized to offsets in fertilized eggs, changed throughout their development in a linear fashion (Fig. 7B), although the direction of the change varied (Fig. 7B). Values of $\Delta^{15}N_{Glx\text{-}Phe}$ ($F_{1,10} = 21.36$, $r^2 = 0.68$, $p < 0.001$) and $\Delta^{15}N_{Glx\text{-}Lys}$ ($F_{1,10} = 18.67$, $r^2 = 0.65$, $p = 0.002$) declined by ~ 2‰, as embryo length increased (Fig. 7B). In

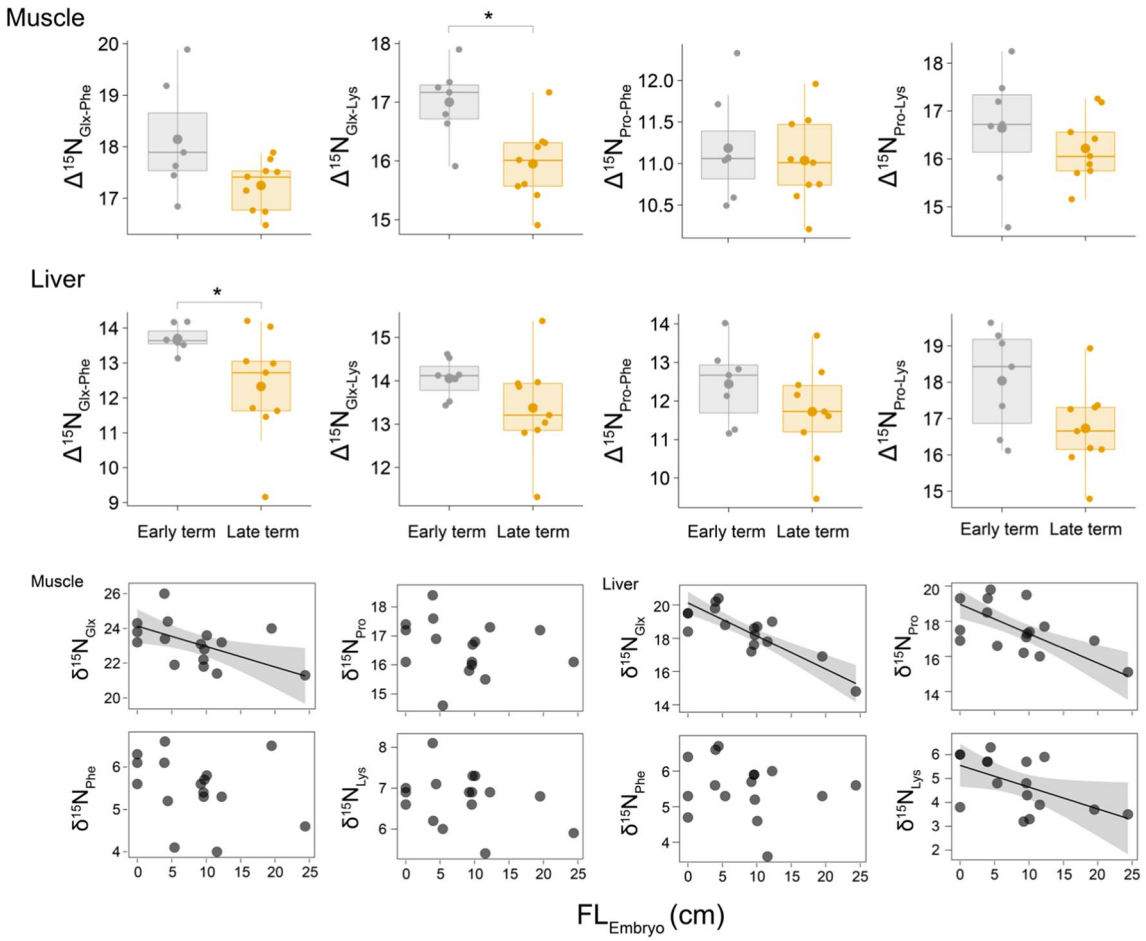

Fig. 4 *Top color panels*: box and whisker plots highlighting offsets between trophic and source amino acids ($\Delta^{15}N_{T\text{-}S}$) for muscle and liver tissue sampled from early-term (gray) and late-term (orange) female bonnethead sharks. Horizontal lines represent median values and large circles represent the mean, boxes display 25th and 75th percentiles and whiskers represent upper and lower quartiles ± 1.5*IQR, remaining points are outliers, and stars represent statistically significant differences as α = 0.05 level. *Bottom panels*: generalized linear model predictions illustrating the relationship between $\delta^{15}N$ values of representative trophic and source amino acids and FL_{Embryo} for muscle (left four panels) and liver (right four panels). Best fit line and 95% CIs are shown for significant relationships at alpha = 0.05 level (see Table 2)

contrast, $\Delta^{15}N_{Pro\text{-}Phe}$ ($F_{1,10} = 64.66$, $r^2 = 0.87$, $p < 0.001$) and $\Delta^{15}N_{Pro\text{-}Lys}$ ($F_{1,10}$, $r^2 = 0.91$, $p < 0.001$) increased by ~ 8‰, as embryo length increased (Fig. 7B).

Discussion

Bulk tissue and AA $\delta^{15}N$ values generally decreased between early- and late-term pregnant female bonnethead sharks. This trend was more prevalent in liver than in muscle, assumingly due liver being a hub of metabolic activity, which results in higher isotopic incorporation rates relative to muscle (MacNeil et al. 2006; Kim et al. 2012; Galvan et al. 2016). We also observed contrasting shifts in $\delta^{15}N$ values of embryo tissues, which generally had higher $\delta^{15}N$ values at later stages of development. Despite a moderate sample size for both bonnethead adults and their pups, these findings illustrate the potential of AA $\delta^{15}N$ values for evaluating potential shifts to nitrogen balance strategies of consumers during nitrogen-demanding life history events (e.g., reproduction), which are discussed below.

Drivers of bulk and AA $\delta^{15}N$ values in pregnant bonnethead sharks

We observed a decline in $\delta^{15}N$ values for both bulk tissues (muscle and liver) and their constituent AAs with advanced gestational stage in female bonnethead sharks. We attribute these isotopic effects to physiological adjustments in response to increasing nitrogen demand after the formation of the yolk-sac placenta to support later-term embryos (i.e., $FL_{Embryo} = 9 - 10$ cm). It has been hypothesized that isotope

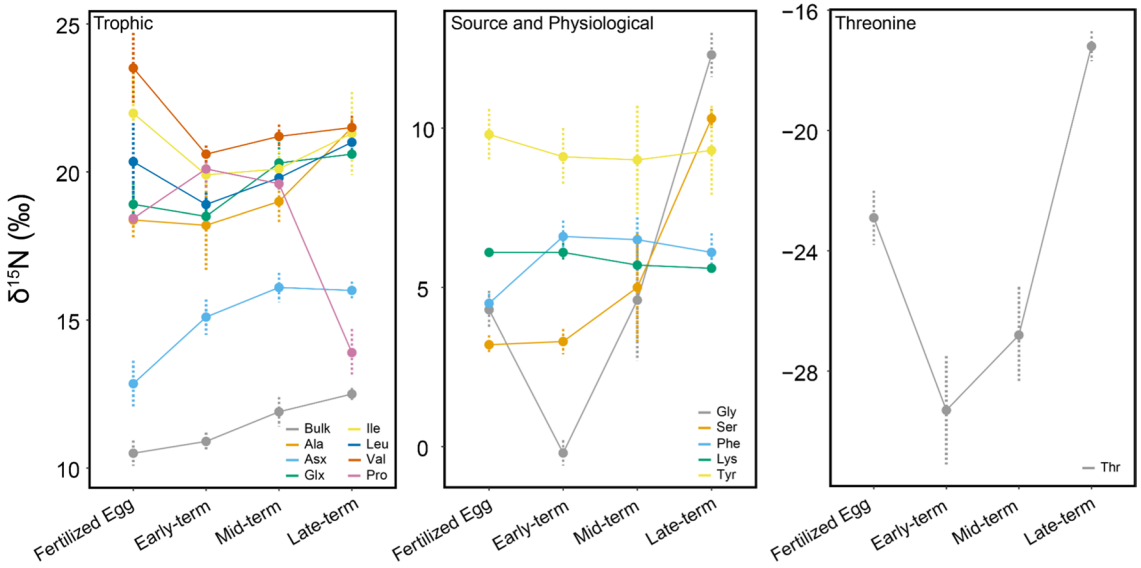

Fig. 5 Changes in bulk tissue and amino acid $\delta^{15}N$ values across bonnethead shark fertilized egg, early-term (whole body tissue), mid-term (liver tissue), and late-term (liver tissue) embryos. Panels are grouped based on their relative application to ecophysiological studies: trophic and bulk tissue (left panel), source and physiological (middle panel), and threonine (right panel)

effects stemming from either dietary or physiological variability, such as switching between two isotopically distinct diets or from exogenous to endogenous resource use, may be more readily reflected in trophic AA $\delta^{15}N$ values (Lübcker et al. 2020b). Trophic AAs (e.g., Glx, Ala, Asx, Leu, Ile, Val, Pro) undergo significant trans- and deamination throughout biosynthesis, many of which (with the exception of Pro) include an α-nitrogen that is interchangeable and closely linked to Glx, the hub of nitrogen cycling in organisms (O'Connell 2017). However, for bonnethead sharks, we observed similar patterns of ^{15}N depletion across many of the trophic (Ala, Glu, Ile, Leu, Val, and Pro), source (Tyr, Lys), and physiological (Gly) AAs. The opposing trends in $\delta^{15}N$ values during prolonged gestation (i.e., progressively lower $\delta^{15}N$ values), in comparison to starvation-induced tissue catabolism typically associated with ^{15}N-enrichment (Hobson et al.1993; Lee et al. 2012; Lübcker et al. 2020b), suggests that the nitrogen demands of reproduction may elicit a relatively unique physiologically-mediated isotopic response (Fuller et al. 2004; Borrell et al. 2016).

Several physiological strategies for maintaining nitrogen balance may drive ^{15}N-depleted bulk tissue and AA $\delta^{15}N$ values in the tissues of pregnant bonnethead sharks in late stages of gestation. First, nitrogen conservation/sparing is a physiological strategy employed by a diverse array of animal taxa, including humans, during periods of high nutritional demand (Pastor-Anglada and Remesar, 1986; King, 2000; Fuller et al. 2005). Nitrogenous waste products (e.g., ammonia, urea, and uric acid) that are depleted in ^{15}N relative to body tissues are retained rather than excreted, providing nitrogen that can instead be recycled via symbiotic, urealytic bacteria (see below) back into the metabolic nitrogen pool (Sponheimer et al. 2003; Fuller et al. 2004). Elasmobranchs primarily excrete nitrogenous waste in the form of urea (~90%, Wood et al. 1995; Kajimura et al. 2008), with a minor fraction in the form of other nitrogen-bearing compounds such as ammonia (Wright 1995; Kijamura et al. 2008). Increased urea retention and nitrogen recycling during advanced stages of bonnethead shark gestation could lead to the routing of conserved ^{14}N into AA synthesis, as suggested in pregnant humans (Fuller et al. 2004).

Second, urealytic bacteria (e.g., *Vibrio* sp.) commonly found in tissues such as chime/intestinal fluid, intestinal epithelial cells (Wood et al. 2019), kidneys, liver, spleen, and pancreas (Grimes et al. 1985; Knight et al. 1988) are suggested to be a primary modulator of urea fluxes in elasmobranchs by catabolizing urea to free ammonia (NH_3) that can be directly routed back to the metabolic nitrogen pool (Wood et al. 2019). Due to the lighter nitrogen isotope composition of urea relative to exogenous and endogenous proteins (Carlisle et al. 2017), increased recycling of urea-N during later gestation could drive lower $\delta^{15}N$ values in female bonnethead shark tissues. If the remobilization of free ammonia from the microbial breakdown of urea is, at least in part, responsible for driving the low $\delta^{15}N$ values observed in later-term sharks, an important trade-off must be managed between the maintenance of urea concentrations for osmoregulation versus AA synthesis to fuel embryo development (Kajimura et al. 2008). This process, however, could explain the decline in $\delta^{15}N$ values of several source AAs, such as Tyr and Lys, which are not typically linked to the metabolic nitrogen pool (O'Connell 2017). A third

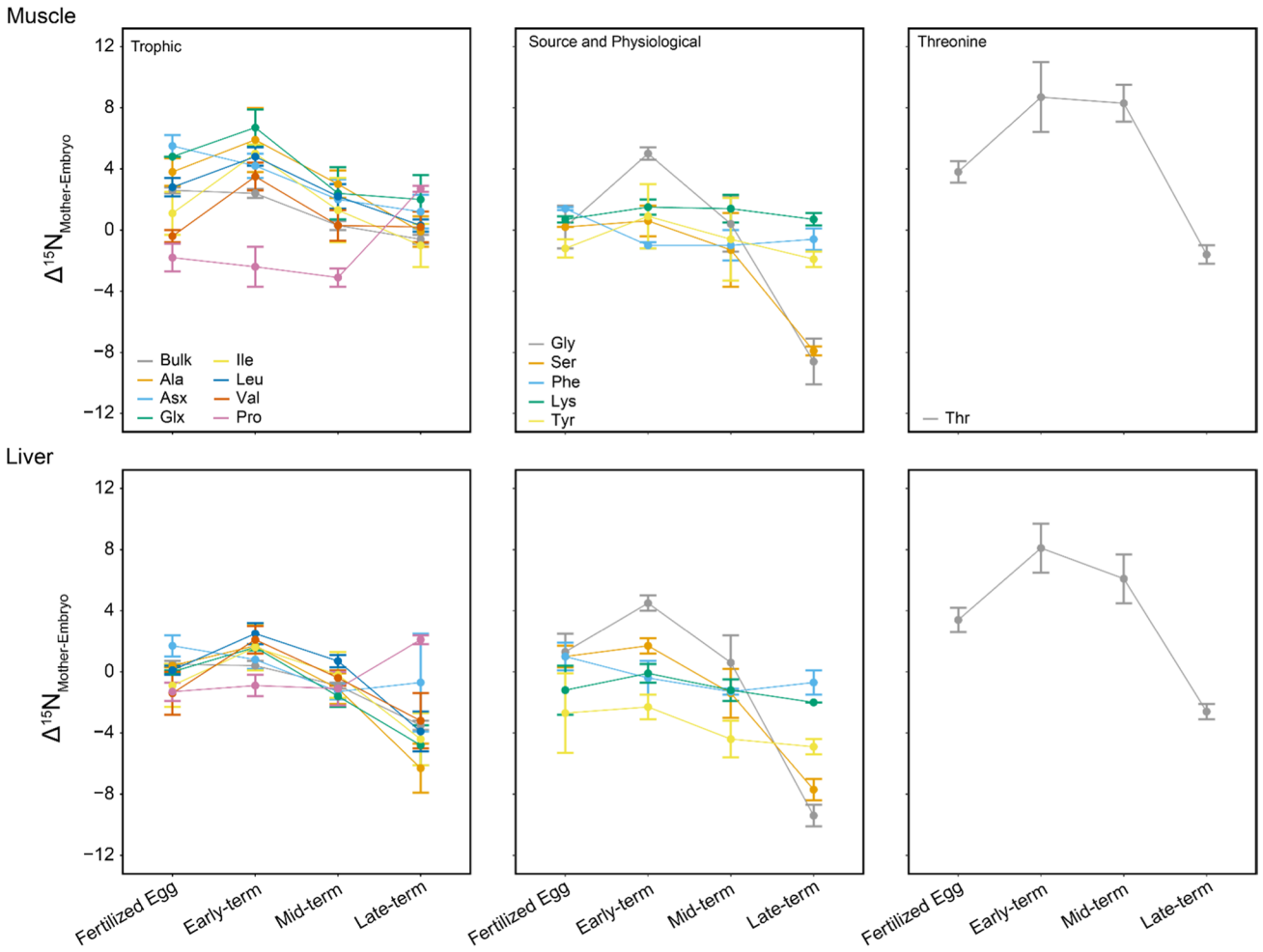

Fig. 6 Bulk tissue and amino acid offsets ($\Delta^{15}N$) between mother muscle (top panels) and liver (bottom panels) tissue with corresponding embryos at four stages of development: fertilized egg ($n=2$), early-term ($n=4$), mid-term ($n=4$), and late-term ($n=4$). Note that isotope data for early-term individuals are based on whole body tissues, whereas mid- and late-term estimates are based on embryo liver tissues

mechanism that may drive the lower $\delta^{15}N$ values in bonnethead sharks at later stages of gestation is the scavenging of nitrogen from ammonia (NH_3) from the surrounding water column via the gill tissue. This strategy has been documented in spiny dogfish (*Squalus acanthias*) and was predicted to reconstitute up to 31% of an individual's dietary nitrogen requirements (Wood and Giacomin 2016). In bonnethead sharks, ammonia-derived ^{14}N could be assimilated into glutamine via the enzyme glutamine synthetase or glutamate via the enzyme glutamate dehydrogenase or glutamate synthase, and then converted to urea through the ornithine–urea cycle (Ballantyne 1997; Wood and Giacomin 2016).

Regardless of the mechanisms driving lower $\delta^{15}N$ values in pregnant females at later stages of gestation, these data provide a basis for hypothesizing about nitrogen dynamics in species displaying alternative reproductive modes. For example, it could be predicted that species exhibiting strict ovipary (egg laying) may be less likely to display a longitudinal pattern in $\delta^{15}N$, given the lack of a direct placental connection with embryos during their development. This is supported by the data presented here, as pregnant bonnethead sharks displayed higher $\delta^{15}N$ values at early stages of gestation during egg formation and maturation. Additionally, it could be predicted that species displaying full vivipary (i.e., placentrophy) may exhibit a sharper decline in $\delta^{15}N$ values throughout gestation, given their constant placental connection to embryos in the absence of stored energetic reserves (as in bonnethead sharks). Although found to be a non-significant predictor of $\delta^{15}N$ values for bonnethead sharks, litter size may also impact the degree of isotopic variation across gestation, with the expectation that larger litters may elicit a higher demand for nitrogen than smaller litters. These hypotheses certainly warrant further investigation,

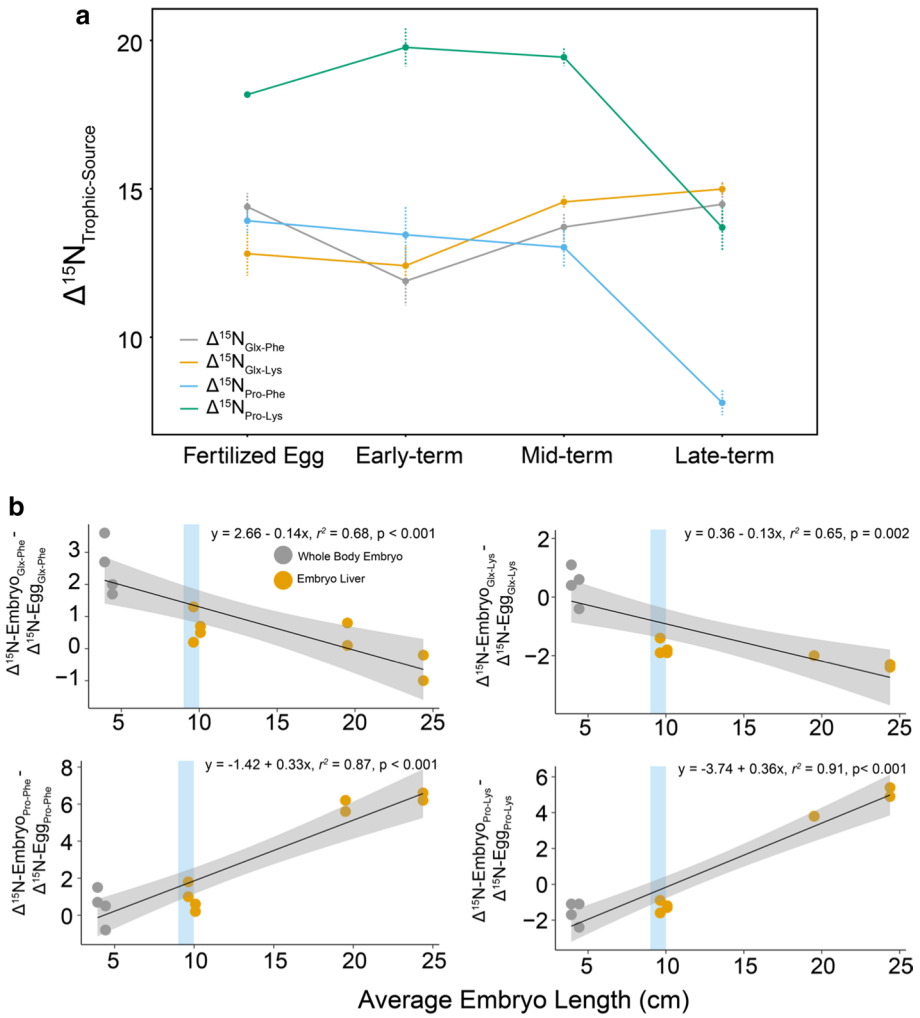

Fig. 7 a Mean (±1 SD) trophic– source pairs for bonnethead fertilized egg embryo tissues across: fertilized egg ($n=2$), early-term ($n=4$, whole body), mid-term ($n=4$, liver), and late-term ($n=4$, liver). b Linear regressions illustrating the relationship between average embryo length (cm) and whole body embryo (grey circles) and embryo liver tissue (orange circles) trophic–source offsets normalized to fertilized egg (Δ^{15}N-Embryo$_{\text{TrophicAA-SourceAA}}$—$\Delta^{15}$ N-Egg-$_{\text{TrophicAA-SourceAA}}$). Vertical shaded blue region represents the length at which embryos typically transition from egg to placental resource use

given previous evidence suggesting differential resource allocation to pups in bonnethead sharks (Olin et al. 2018). While these predictions remain somewhat speculative, identifying whether nitrogen balance strategies are uniform across sharks displaying different reproductive modes would help clarify the ecological interpretation of isotopic variation in elasmobranchs, and vertebrates more generally.

Finally, we must note that variation in isotopic baselines can significantly alter ecological and physiological interpretation of consumer isotope data, especially in coastal ecosystems that can be highly influenced by anthropogenically derived nitrogen (Shipley et al. 2021; Matich et al. 2021). Furthermore, changes in the movements and foraging behavior of animals during gestation is an important topic of interest, as it can illuminate adaptive capacities when faced with energetically challenging life history events like reproduction. While we considered baseline variation as a plausible factor that may influence the isotopic composition of bonnethead sharks, we captured individuals at all stages of gestation at multiple sampling sites, suggesting that baseline variation is an unlikely explanation for the significant decreases in δ^{15}N values over the course of gestation.

Drivers of bulk and AA δ.^{15} N values in bonnethead shark embryos

A longitudinal record of nitrogen isotope dynamics across a range of embryo developmental stages revealed general increases in bulk and AA δ^{15}N values of embryo tissues (either whole body or liver, depending on size; Fig. 5) relative to their corresponding mothers (Fig. 6), in addition to

an increase in $\Delta^{15}N_{Trophic\text{-}Source}$ (Glx-Phe and Glx-Lys) as embryos reached later stages of development (Fig. 7). This enrichment could be explained by an increased rate of nitrogen excretion in later-term embryos, where greater amounts of ^{14}N are preferentially lost during formation of urea; such increasing excretion could reflect the morphological development of kidneys and other structures. Similarly, increased de novo synthesis of non-essential AAs in more developed embryos would reduce the necessity for direct routing via the yolk-sac placenta, again increasing ^{15}N of embryo tissues relative to their mothers.

A particularly notable trend was the large increase in $\delta^{15}N$ values of Gly and Ser in later-term embryos (Fig. 5), which may reflect active nitrogen transport occurring across the fetal placenta via transport system A and activity of the glycine-serine shuttle (Narkewicz et al. 2002; Kalhan 2016), as proposed for fetal elephant seals (Lübcker et al. 2020a). This shuttle and the accompanying demethylation of glycine by the fetal liver provide essential one-carbon units (via *s*-adenoslymethionine) that are required for nucleotide synthesis (Lindsay et al. 2015; Kalhan, 2016). This process likely preferentially deaminates the ^{14}N of amine groups from Gly and Ser to form pyruvate, leaving residual Gly and Ser (used to build tissues) ^{15}N-enriched. During rapid growth of fetal tissue, the high demand for nucleotide synthesis could therefore cause enhanced fractionation of Gly and Ser (Lübcker et al. 2020a). Although data are lacking for many vertebrate taxa, recent studies of emperor penguins (Whiteman et al. 2021a, b) and elephant seals (Lübcker et al. 2020a) also indicate that these two non-essential, glycolytic AAs seem to be sensitive to nitrogen balance. Thus, we hypothesize that metabolic shuttling of nitrogen across the placenta via Gly and Ser could be relatively uniform across species that use placentas to allocate resources to embryos.

A second notable trend was observed for Pro $\delta^{15}N$ values, which were lower in later-term embryos (19 – 25 cm, Figs. 5, 6 & 7). Although proline does not readily exchange alpha nitrogen with glutamic acid, as common with other trophic AAs (O'Connell 2017), its amino nitrogen typically shares the same nitrogen pool as other trophic AAs when synthesized from glutamate. Thus, it would be expected that physiologically mediated isotope patterns related to trophic transfer that are observed in glutamic acid would also be reflected in proline if the predominant biosynthesis pathway of proline is via glutamate. However, proline can also be synthesized from arginine via the ornithine pathway (Delauney et al. 1993; Kishor et al. 2005), whereby amino nitrogen is derived from the urea cycle (Zhang and Becker 2015). Because proline concentration increases significantly in the tissues of developing embryos (Wu et al. 1999; 2010; 2011), it is curious whether an elevated proline demand over the course of gestation results in a change of the predominant biosynthesis pathway shifting from a glutamate to ornithine precursor. Given these pathways, there are two possible mechanisms that could lead to the significant decrease in Pro $\delta^{15}N$ values. First, the isotopic composition of the predominant nitrogen pools supporting the synthesis of proline from glutamate differ from that of arginine/ornithine (Dagenais-Bellefeuille and Morse 2013), which could explain the lower $\delta^{15}N_{Pro}$ values in more developed embryos. An alternative explanation is that fractionation associated with proline synthesis via the ornithine pathway could be significantly lower than that associated with the glutamate pathway, if the isotopic composition of the metabolic nitrogen pool supporting both pathways is the same. Ultimately, the drivers of nitrogen isotope dynamics of proline remain speculative. It is clear, however, that despite being considered a 'trophic' AA, proline has become increasingly utilized as a physiological marker of nitrogen balance in vertebrates (e.g., Whiteman et al. 2021a, b). The trends observed here again suggest that proline may be an important physiological predictor of developmental stage in vertebrate embryos, which would limit its use as a trophic marker in young-of-the-year individuals.

Intriguingly, the trends in Gly, Ser, and Pro discussed above were most dramatic for late-stage embryos. Simultaneously, there was also a convergence of $\delta^{15}N$ values for most remaining trophic AAs (Ala, Glx, Ile, Leu, Val), which could indicate rapid embryonic growth enhancing cycling of nitrogen through all biochemical pathways connected to the central metabolic pool, effectively homogenizing the resulting fractionation.

Conclusions

This study illustrates strong linkages between reproduction and bulk tissue and AA isotopic composition of adult females and their respective embryos. Much of the isotopic variation observed in pregnant female sharks was explained by gestational stage, suggesting fractionation during pregnancy could be a first-order control on isotopic variability, at least for female elasmobranchs. Similarly, variation in embryo $\delta^{15}N$ values was closely tied to developmental stage reflecting potential shifts from direct routing of AAs to greater de novo synthesis, in addition to greater excretion of ^{14}N-rich waste. Given that isotopic spacing between trophic and source AAs (e.g., $\delta^{15}N_{Glu\text{-}Phe,}$ and $\delta^{15}N_{Pro\text{-}Phe}$ etc.) is typically used to determine estimates of animal trophic position (Nielsen et al. 2015; McMahon and McCarthy 2016; Ohkouchi et al. 2017), and food-chain length (Ruiz-Cooley et al. 2017; Chua et al.2021), isotopic variability associated with shifting nitrogen balance strategies may confound the accurate ecological interpretation of $\delta^{15}N$ values in consumers

(Lübcker et al. 2020a, b), at least for tissues with fast isotopic incorporation rates. Given the clear and relatively unique patterns of isotopic depletion associated with mature females at advanced stages of gestation, it is possible that additional statistical techniques, such as linear discriminant analyses, could be utilized to predict gestational stage for unknown individuals based on AA $\delta^{15}N$ values alone. However, this robust statistical approach would require a higher sample size than presented here. Our results emphasize that future studies aiming to assess ecological patterns using bulk and amino acid nitrogen isotopes should consider reproductive status, nitrogen balance, and other physiological conditions at the time of sampling.

Supplementary Information The online version contains supplementary material available at https://doi.org/10.1007/s00442-022-05197-6.

Acknowledgements The authors would like to thank S. Farr, P. Manlick, N. Lübcker, G. Busquets-Vass, L. Burkemper, and V. Atudorei for laboratory assistance. We are grateful to the NOAA Fisheries Panama City Laboratory Shark Population Assessment Group, especially B. Burleson, G. Casselberry, J. Clayton, D. DeLorenzo, S. Dunnigan, E. Heikkinen, P. Higginson, R. Jones, C. Larash, B. Meath, A. Mowle, A. Pacicco, R. Peters, C. Rewis, and H. Wood for volunteering time to help collect and process samples in the field and laboratory. We are also grateful for the input received from anonymous reviewers that greatly improved the manuscript.

Author contribution statement ONS, JAO, JPW, and SDN conceived the project ideas and designed the methodology. JAO and DB conducted fieldwork and collected samples. ONS and SDN conducted laboratory analyses and analyzed the data. ONS led the writing of the manuscript with significant input from all authors. All authors approved the final version of the manuscript.

Data availability Data will be uploaded to the only repository IsoBank (www.isobank.org) upon acceptance for publication.

Declarations

Conflict of interest The authors declare no conflict of interest.

References

Ballantyne JS (1997) Jaws: the inside story. The metabolism of elasmobranch fishes. Comp Biochem Physiol B: Biochem Mol Biol 118(4):703–742

Ballantyne JS (2016) Some of the most interesting things we know, and don't know, about the biochemistry and physiology of elasmobranch fishes (sharks, skates and rays). Comp Biochem Physiol B: Biochem Mol Biol 199:21–28

Baremore IE, Hale LF (2012) Reproduction of the sandbar shark in the western north Atlantic ocean and Gulf of Mexico. Mar Coast Fish: Dyn Manag Ecosyst Sci 4:560–572

Barnes C, Sweeting CJ, Jennings S, Barry JT, Polunin NV (2007) Effect of temperature and ration size on carbon and nitrogen stable isotope trophic fractionation. Funct Ecol 21(2):356–362

Bethea DM, Hale L, Carlson JK, Cortés E, Manire CA, Gelsleichter J (2007) Geographic and ontogenetic variation in the diet and daily ration of the bonnethead shark, Sphyrna tiburo, from the eastern Gulf of Mexico. Mar Biol 152(5):1009–1020

Bethea, D.M., G.A. Casselberry, J.K. Carlson, J. Hendon, R.D. Grubbs, C. Peterson, T.S. Daly-Engel, M.O. Pfleger, R. Hueter, J. Morris, J. Gardiner (2016) Shark nursery grounds and essential fish habitat studies. Gulfspan Gulf of Mexico-FY15. An Internal Report to NOAA Fisheries Highly Migratory Species Division. NMFS Panama City Laboratory Contribution No. PC-16/02.

Boecklen WJ, Yarnes CT, Cook BA, James AC (2011) On the use of stable isotopes in trophic ecology. Annu Rev Ecol Evol Syst 42:411–440

Borrell A, Gómez-Campos E, Aguilar A (2016) Influence of reproduction on stable-isotope ratios: nitrogen and carbon isotope discrimination between mothers, fetuses, and milk in the fin whale, a capital breeder. Physiol Biochem Zool 89(1):41–50

Bryan HM, Darimont CT, Paquet PC, Wynne-Edwards KE, Smits JE (2013) Stress and reproductive hormones in grizzly bears reflect nutritional benefits and social consequences of a salmon foraging niche. PLoS ONE 8(11):e80537

Carlisle AB, Litvin SY, Madigan DJ, Lyons K, Bigman JS, Ibarra M, Bizzarro JJ (2017) Interactive effects of urea and lipid content confound stable isotope analysis in elasmobranch fishes. Can J Fish Aquat Sci 74(3):419–428

Carlson JK, Brusher JH (1999) An Index of Abundance for coastal species of Juvenile sharks from the northeast Gulf of Mexico. Mar Fish Rev 61(3):37–45

Chua KW, Liew JH, Wilkinson CL, Ahmad AB, Tan HH, Yeo DC (2021) Land-use change erodes trophic redundancy in tropical forest streams: evidence from amino acid stable isotope analysis. J Anim Ecol 90(6):1433–1443

Clark CT, Fleming AH, Calambokidis J, Kellar NM, Allen CD, Catelani KN, Harvey JT (2016) Heavy with child? Pregnancy status and stable isotope ratios as determined from biopsies of humpback whales. Conser Physiol 4(1):1–13

Conrath CL, Musick JA (2012) Reproductive biology of elasmobranchs. In: Biology of sharks and their relatives, vol 2, pp 291–311

Cortés E (2000) Life history patterns and correlations in sharks. Rev Fish Sci 8(4):299–344

Dagenais-Bellefeuille S, Morse D (2013) Putting the N in dinoflagellates. Front Microbiol 4:369

de Sousa Rangel B, Hammerschlag N, Sulikowski JA, Moreira RG (2021) Dietary and reproductive biomarkers in a generalist apex predator reveal differences in nutritional ecology across life stages. Mar Ecol Prog Ser 664:149–163

Delauney AJ, Hu CA, Kishor PB, Verma DP (1993) Cloning of ornithine delta-aminotransferase cDNA from Vigna aconitifolia by trans-complementation in Escherichia coli and regulation of proline biosynthesis. J Biol Chem 268(25):18673–18678

Dulvy NK, Fowler SL, Musick JA, Cavanagh RD, Kyne PM, Harrison LR, White WT (2014) Extinction risk and conservation of the world's sharks and rays. Elife 3:00590

Estrada JA, Rice AN, Natanson LJ, Skomal GB (2006) Use of isotopic analysis of vertebrae in reconstructing ontogenetic feeding ecology in white sharks. Ecology 87(4):829–834

Evans RD (2001) Physiological mechanisms influencing plant nitrogen isotope composition. Trends Plant Sci 6(3):121–126

Fleming AH, Kellar NM, Allen CD, Kurle CM (2018) The utility of combining stable isotope and hormone analyses for marine megafauna research. Front Mar Sci 5:338

Folch J (1957) A sample method for the isolation and purification of total lipids from animal tissues. J Biol Chem 226:479–500

Frisk MG, Miller TJ, Dulvy NK (2005) Life histories and vulnerability to exploitation of elasmobranchs: inferences from elasticity,

perturbation and phylogenetic analyses. J Northwest Atl Fish Sci 35:27–45
Fuller BT, Fuller JL, Sage NE, Harris DA, O'Connell TC, Hedges RE (2004) Nitrogen balance and δ15N: why you're not what you eat during pregnancy. Rapid Commun Mass Spectrom 18(23):2889–2896
Fuller BT, Fuller JL, Sage NE, Harris DA, O'Connell TC, Hedges RE (2005) Nitrogen balance and $\delta^{15}N$: why you're not what you eat during nutritional stress. Rapid Commun Mass Spectrom 19(18):2497–2506
Gallagher AJ, Skubel RA, Pethybridge HR, Hammerschlag N (2017) Energy metabolism in mobile, wild-sampled sharks inferred by plasma lipids. Conserv Physiol. https://doi.org/10.1093/conphys/cox002
Galvan DE, Sweeting CJ, Reid WDK (2010) Power of stable isotope techniques to detect size-based feeding in marine fishes. Mar Ecol Prog Ser 407:271–278
Galvan DE, Jañez J, Irigoyen AJ (2016) Estimating tissue-specific discrimination factors and turnover rates of stable isotopes of nitrogen and carbon in the smallnose fanskate *Sympterygia bonapartii* (Rajidae). J Fish Biol 89(2):1258–1270
Gannes LZ, Del Rio CM, Koch P (1998) Natural abundance variations in stable isotopes and their potential uses in animal physiological ecology. Comp Biochem Physiol a: Mol Integr Physiol 119(3):725–737
Gorokhova E (2018) Individual growth as a non-dietary determinant of the isotopic niche metrics. Methods Ecol Evol 9(2):269–277
Graves GR, Newsome SD, Willard DE, Grosshuesch DA, Wurzel WW, Fogel ML (2012) Nutritional stress and body condition in the Great Gray Owl (Strix nebulosa) during winter irruptive migrations. Can J Zool 90(7):787–797
Grimes DJ, Brayton P, Colwell RR, Gruber SH (1985) Vibrios as autochthonous flora of neritic sharks. Syst Appl Microbiol 6(2):221–226
Hamlett WC, Jones CJP, Paulesu LR (2005) Placentotrophy in sharks. In: Hamlett WC, Jamieson BGM (eds) Reproductive biology and phylogeny. Science publishers Inc., NH, pp 463–502
Hammerschlag N, Skubel RA, Sulikowski J, Irschick DJ, Gallagher AJ (2018) A comparison of reproductive and energetic states in a marine apex predator (the tiger shark, Galeocerdo cuvier). Physiol Biochem Zool 91(4):933–942
Hebert CE, Popp BN, Fernie KJ, Ka'apu-Lyons C, Rattner BA, Wallsgrove N (2016) Amino acid specific stable nitrogen isotope values in avian tissues: insights from captive American kestrels and wild herring gulls. Environ Sci Technol 50(23):12928-12937
Hobson KA, Alisauskas RT, Clark RG (1993) Stable-nitrogen isotope enrichment in avian tissues due to fasting and nutritional stress: implications for isotopic analyses of diet. The Condor 95(2):388–394
Hussey NE, Olin JA, Kinney MJ, McMeans BC, Fisk AT (2012) Lipid extraction effects on stable isotope values ($\delta^{13}C$ and $\delta^{15}N$) of elasmobranch muscle tissue. J Exp Mar Biol Ecol 434:7–15
Kajimura M, Walsh PJ, Wood CM (2008) The spiny dogfish *Squalus acanthias* L. maintains osmolyte balance during long-term starvation. J Fish Biol 72(3):656–670
Kalhan SC (2016) One carbon metabolism in pregnancy: Impact on maternal, fetal and neonatal health. Mol Cell Endocrinol 435:48–60
Kim SL, Martínez del Rio C, Casper D, Koch PL (2012) Isotopic incorporation rates for shark tissues from a long-term captive feeding study. J Exp Biol 215:2495–2500
King JC (2000) Physiology of pregnancy and nutrient metabolism. Am J Clin Nutr 71(5):1218S-1225S
Kishor PK, Sangam S, Amrutha RN, Laxmi PS, Naidu KR, Rao KRSS, Sreenath Rao, Reddy KJ, Theriappan P, Sreenivasulu N (2005) Regulation of proline biosynthesis, degradation, uptake and transport in higher plants: its implications in plant growth and abiotic stress tolerance. Curr Sci 88:424–438
Knight IT, Grimes DJ, Colwell RR (1988) Bacterial hydrolysis of urea in the tissues of carcharhinid sharks. Can J Fish Aquat Sci 45(2):357–360
Kounig B, Riester J, Markl H (1988) Maternal care in house mice (Mus musculus) II. The energy cost of lactation as a function of litter size. J Zool 216(2):195–210
Kouwenberg AL, Mark Hipfner J, McKay DW, Storey AE (2013) Corticosterone and stable isotopes in feathers predict egg size in A tlantic P uffins F ratercula arctica. Ibis 155(2):413–418
Larsen T, Taylor DL, Leigh MB, O'Brien DM (2009) Stable isotope fingerprinting: a novel method for identifying plant, fungal, or bacterial origins of amino acids. Ecology 90(12):3526–3535
Laxson CJ, Condon NE, Drazen JC, Yancey PH (2011) Decreasing urea: trimethylamine N-oxide ratios with depth in chondrichthyes: a physiological depth limit? Physiol Biochem Zool 84(5):494–505
Layman CA, Araujo MS, Boucek R, Hammerschlag-Peyer CM, Harrison E, Jud ZR, Bearhop S (2012) Applying stable isotopes to examine food-web structure: an overview of analytical tools. Biol Rev 87(3):545–562
Lee TN, Buck CL, Barnes BM, O'Brien DM (2012) A test of alternative models for increased tissue nitrogen isotope ratios during fasting in hibernating arctic ground squirrels. J Exp Biol 215(19):3354–3361
Leigh SC, Papastamatiou YP, German DP (2018) Seagrass digestion by a notorious "carnivore." Proc R Soc B 285:20181583
Leon M, Woodside B (1983) Energetic limits on reproduction: maternal food intake. Physiol Behav 30(6):945–957
Lindsay KL, Hellmuth C, Uhl O, Buss C, Wadhwa PD, Koletzko B, Entringer S (2015) Longitudinal metabolomic profiling of amino acids and lipids across healthy pregnancy. PLoS ONE 10(12):e0145794
Lübcker N, Whiteman JP, Millar RP, de Bruyn PN, Newsome SD (2020) Fasting affects amino acid nitrogen isotope values: a new tool for identifying nitrogen balance of free-ranging mammals. Oecologia 193(1):53–65
Lübcker N, Whiteman JP, Newsome SD, Millar RP, de Bruyn PN (2020) Can the carbon and nitrogen isotope values of offspring be used as a proxy for their mother's diet? Using foetal physiology to interpret bulk tissue and amino acid δ15N values. Conserv Physiol. https://doi.org/10.1093/conphys/coaa060
MacNeil MA, Drouillard KG, Fisk AT (2006) Variable uptake and elimination of stable nitrogen isotopes between tissues in fish. Can J Fish Aquat Sci 63(2):345–353
Matich P, Kiszka JJ, Heithaus MR, Le Bourg B, Mourier J (2019) Interindividual differences in ontogenetic trophic shifts among three marine predators. Oecologia 189(3):621–636
Matich P, Shipley ON, Wiedeli O (2021) Quantifying spatial variation in isotopic baselines reveals size-based feeding in a model estuarine predator: implications for trophic studies in dynamic ecotones. Mar Biol. https://doi.org/10.1007/s00227-021-03920-0
McConnaughey T, McRoy CP (1979) Food-web structure and the fractionation of carbon isotopes in the Bering Sea. Mar Biol 53(3):257–262
McMahon KW, McCarthy MD (2016) Embracing variability in amino acid δ15N fractionation: mechanisms, implications, and applications for trophic ecology. Ecosphere 7(12):e01511
McMahon KW, Thorrold SR, Elsdon TS, McCarthy MD (2015) Trophic discrimination of nitrogen stable isotopes in amino acids varies with diet quality in a marine fish. Limnol Oceanogr 60(3):1076–1087
McMeans BC, Olin JA, Benz GW (2009) Stable-isotope comparisons between embryos and mothers of a placentatrophic shark species. J Fish Biol 75(10):2464–2474

Narkewicz MR, Jones G, Thompson H, Kolhouse F, Fennessey PV (2002) Folate cofactors regulate serine metabolism in fetal ovine hepatocytes. Pediatr Res 52(4):589–594

Nielsen JM, Popp BN, Winder M (2015) Meta-analysis of amino acid stable nitrogen isotope ratios for estimating trophic position in marine organisms. Oecologia 178(3):631–642

O'Connell T (2017) 'Trophic'and 'source'amino acids in trophic estimation: a likely metabolic explanation. Oecologia 184(2):317–326

Ohkouchi N, Chikaraishi Y, Close HG, Fry B, Larsen T, Madigan DJ, Yokoyama Y (2017) Advances in the application of amino acid nitrogen isotopic analysis in ecological and biogeochemical studies. Org Geochem 113:150–174

Olin JA, Hussey NE, Fritts M, Heupel MR, Simpfendorfer CA, Poulakis GR, Fisk AT (2011) Maternal meddling in neonatal sharks: implications for interpreting stable isotopes in young animals. Rapid Commun Mass Spectrom 25(8):1008–1016

Olin JA, Shipley ON, McMeans BC (2018) Stable isotope fractionation between maternal and embryo tissues in the Bonnethead shark (Sphyrna tiburo). Environ Biol Fishes 101(3):489–499

Pastor-Anglada M, Remesar X (1986) Urinary amino acid excretion in the pregnant rat. Nutr Res 6(6):709–718

Ruiz-Cooley RI, Gerrodette T, Fiedler PC, Chivers SJ, Danil K, Ballance LT (2017) Temporal variation in pelagic food chain length in response to environmental change. Sci Adv 3(10):1701140

Schlernitzauer DA, Gilbert PW (1966) Placentation and associated aspects of gestation in the bonnethead shark, Sphyrna tiburo. J Morphol 120(3):219–231

Silfer JA, Engel MH, Macko SA, Jumeau EJ (1991) Stable carbon isotope analysis of amino acid enantiomers by conventional isotope ratio mass spectrometry and combined gas chromatography/isotope ratio mass spectrometry. Anal Chem 63(4):370–374

Shipley ON, Matich P (2020) Studying animal niches using bulk stable isotope ratios: an updated synthesis. Oecologia 193:27–51

Shipley ON, Olin JA, Polunin NV, Sweeting CJ, Newman SP, Brooks EJ, Hussey NE (2017) Polar compounds preclude mathematical lipid correction of carbon stable isotopes in deep-water sharks. J Exp Mar Biol Ecol 494:69–74

Shipley ON, Brooks EJ, Madigan DJ, Sweeting CJ, Grubbs RD (2017) Stable isotope analysis in deep-sea chondrichthyans: recent challenges, ecological insights, and future directions. Rev Fish Biol Fisheries 27(3):481–497

Shipley ON, Newton AL, Frisk MG, Henkes GA, LaBelle JS, Camhi MD, Olin JA (2021) Telemetry-validated nitrogen stable isotope clocks identify ocean-to-estuarine habitat shifts in mobile organisms. Methods Ecol Evol 12(5):897–908

Skinner C, Mill AC, Fox MD, Newman SP, Zhu Y, Kuhl A, Polunin NVC (2021) Offshore pelagic subsidies dominate carbon inputs to coral reef predators. Sci Adv 7(8):eabf3792

Smith HW (1936) The retention and physiological role of urea in the Elasmobranchii. Biol Rev 11(1):49–82

Smith HW, James PB, Herbert S (1929) The composition of the body fluids of elasmobranchs. J Biol Chem 81(2):407–419

Sponheimer M, Robinson T, Ayliffe L, Roeder B, Hammer J, Passey B, Ehleringer J (2003) Nitrogen isotopes in mammalian herbivores: hair δ15N values from a controlled feeding study. Int J Osteoarchaeol 13(1–2):80–87

Stein RW, Mull CG, Kuhn TS, Aschliman NC, Davidson LN, Joy JB, Smith GJ, Dulvy NK, Mooers AO (2018) Global priorities for conserving the evolutionary history of sharks, rays and chimaeras. Nat Ecol Evol 2(2):288–298

Sweeting CJ, Polunin NVC, Jennings S (2006) Effects of chemical lipid extraction and arithmetic lipid correction on stable isotope ratios of fish tissues. Rapid Commun Mass Spectrom 20(4):595–601

Tieszen LL, Boutton TW, Tesdahl KG, Slade NA (1983) Fractionation and turnover of stable carbon isotopes in animal tissues: implications for δ13C analysis of diet. Oecologia 57(1–2):32–37

Whiteman JP, Kim SL, McMahon KW, Koch PL, Newsome SD (2018) Amino acid isotope discrimination factors for a carnivore: physiological insights from leopard sharks and their diet. Oecologia 188(4):977–989

Whiteman JP, Elliott Smith EA, Besser AC, Newsome SD (2019) A guide to using compound-specific stable isotope analysis to study the fates of molecules in organisms and ecosystems. Diversity 11(1):8

Whiteman JP, Newsome SD, Bustamante P, Cherel Y, Hobson KA (2021) Quantifying capital versus income breeding: new promise with stable isotope measurements of individual amino acids. J Anim Ecol 90(6):1408–1418

Whiteman JP, Rodriguez Curras M, Feeser KL, Newsome SD (2021) Dietary protein content and digestibility influences discrimination of amino acid nitrogen isotope values in a terrestrial omnivorous mammal. Rapid Commun Mass Spectrom 35(11):e9073

Widdowson EM (1976) The response of the sexes to nutritional stress. Proc Nutr Soc 35(2):175–180

Wood CM, Giacomin M (2016) Feeding through your gills and turning a toxicant into a resource: how the dogfish shark scavenges ammonia from its environment. J Exp Biol 219(20):3218–3226

Wood CM, Pärt P, Wright PA (1995) Ammonia and urea metabolism in relation to gill function and acid-base balance in a marine elasmobranch, the spiny dogfish (*Squalus acanthias*). J Exp Biol 198(7):1545–1558

Wood CM, Liew HJ, De Boeck G, Hoogenboom JL, Anderson WG (2019) Nitrogen handling in the elasmobranch gut: a role for microbial urease. J Exp Biol 222(3):jeb194787

Wright PA (1995) Nitrogen excretion: three end products, many physiological roles. J Exp Biol 198(2):273–281

Wu G, Ott TL, Knabe DA, Bazer FW (1999) Amino acid composition of the fetal pig. J Nutr 129(5):1031–1038

Wu G, Bazer FW, Burghardt RC, Johnson GA, Kim SW, Knabe DA, Spencer TE (2010) Functional amino acids in swine nutrition and production. Dyn Anim Nutr 69:98

Wu G, Bazer FW, Burghardt RC, Johnson GA, Kim SW, Knabe DA, Spencer TE (2011) Proline and hydroxyproline metabolism: implications for animal and human nutrition. Amino Acids 40(4):1053–1063

Zhang L, Becker D (2015) Connecting proline metabolism and signaling pathways in plant senescence. Front Plant Sci 6:552